ELSEVIER

Journal of Biomechanics 33 (2000) 367–373

JOURNAL OF BIOMECHANICS

www.elsevier.com/locate/jbiomech

Technical Note

Constitutive modelling of abdominal organs

Karol Miller*

Department of Mechanical and Materials Engineering, The University of Western Australia, Nedlands/Perth, WA 6907, Australia

Received 28 September 1998; accepted 12 October 1999

Abstract

Abdominal organs are very susceptible to trauma. In order to protect them properly against car crash and other impact consequences, we need to be able to simulate the abdominal organ deformation. Such simulation should account for proper stress–strain relation as well as stress dependence on strain rate. As the step in this direction, this paper presents three-dimensional, non-linear, viscoelastic constitutive models for liver and kidney tissue. The models have been constructed basing on in vivo experiments conducted in Highway Safety Research Institute and the Medical Centre of The University of Michigan (Melvin et al., 1973). The proposed models are valid for compressive nominal strains up to 35% and fast (impact) strain rates between 0.2 and 22.5 s^{-1}. Similar models can find applications in computer and robot assisted surgery, e.g. the realistic simulation of surgical procedures (including virtual reality) and non-rigid registration.

Keywords: Kidney tissue; Liver tissue; Mechanical properties; Mathematical modelling

1. Introduction

The increased requirements for automotive safety demand closer examination of the mechanical properties of abdominal tissues. The accurate tissue models are the perquisites for realistic injury simulation and designing methods for injury prevention. Moreover, recent developments in robotics technology, especially the emergence of automatic surgical tools and robots (e.g. Brett et al., 1995) as well as advances in virtual reality techniques (Burdea, 1996), make the robotic surgery and virtual reality surgeon training and operation planning systems a goal within our reach. Such systems for rigid tissues (see e.g. Journal of Computer Aided Surgery) already exist. Their development for "very" soft tissues is very much dependent on the knowledge of these tissues' mechanical properties and the existence of the appropriate mathematical models.

The reported experimental data on the mechanical properties of liver and kidney are limited. Most of the papers appeared in the medical journals and discussed the types of injuries without direct reference to the mechanics of the organs (e.g. Divicenti et al., 1968; Guerriero, 1993; Hossack, 1972; Huelke et al., 1980; Rouhana et al., 1985; Rutledge et al., 1991). Recently, Farshad et al. (1998) presented in vitro experimental results and a mathematical model of a pig kidney. Schmidlin et al. (1996) proposed a two-dimensional finite element model of the kidney to investigate injury mechanisms in renal trauma. However, a very simple hyperelastic constitutive equation (based on Yamada, 1970) for the tissue was assumed in that paper. As a result, important velocity dependent phenomena (see e.g. "Viscous criterion", Viano et al., 1989a,b; Viano and Lau, 1988) could not be accounted for.

The theoretical results of this paper — the first, to the best of the author's knowledge, three-dimensional, non-linear, viscoelastic constitutive models of liver and kidney — are based on the results of in vivo experiments on Rhesus monkeys (Melvin et al., 1973). We attempt to prove that the non-linear viscoelastic model, based on the strain energy function in polynomial form with time dependent coefficients, is suitable for description of liver and kidney tissue deformation behaviour under compression, at high strain rates, typical for impact loading.

2. Stress–strain relationship for liver and kidney

Melvin et al. (1973) conducted in vivo constant velocity compression tests on 17 livers and six kidneys of anaesthetised Rhesus monkeys. Results of these tests form, to

* Fax: +61-8-9380-1024.
E-mail address: kmiller@mech.uwa.edu.au (K. Miller)

0021-9290/00/$ - see front matter
PII: S0021-9290(99)00196-7

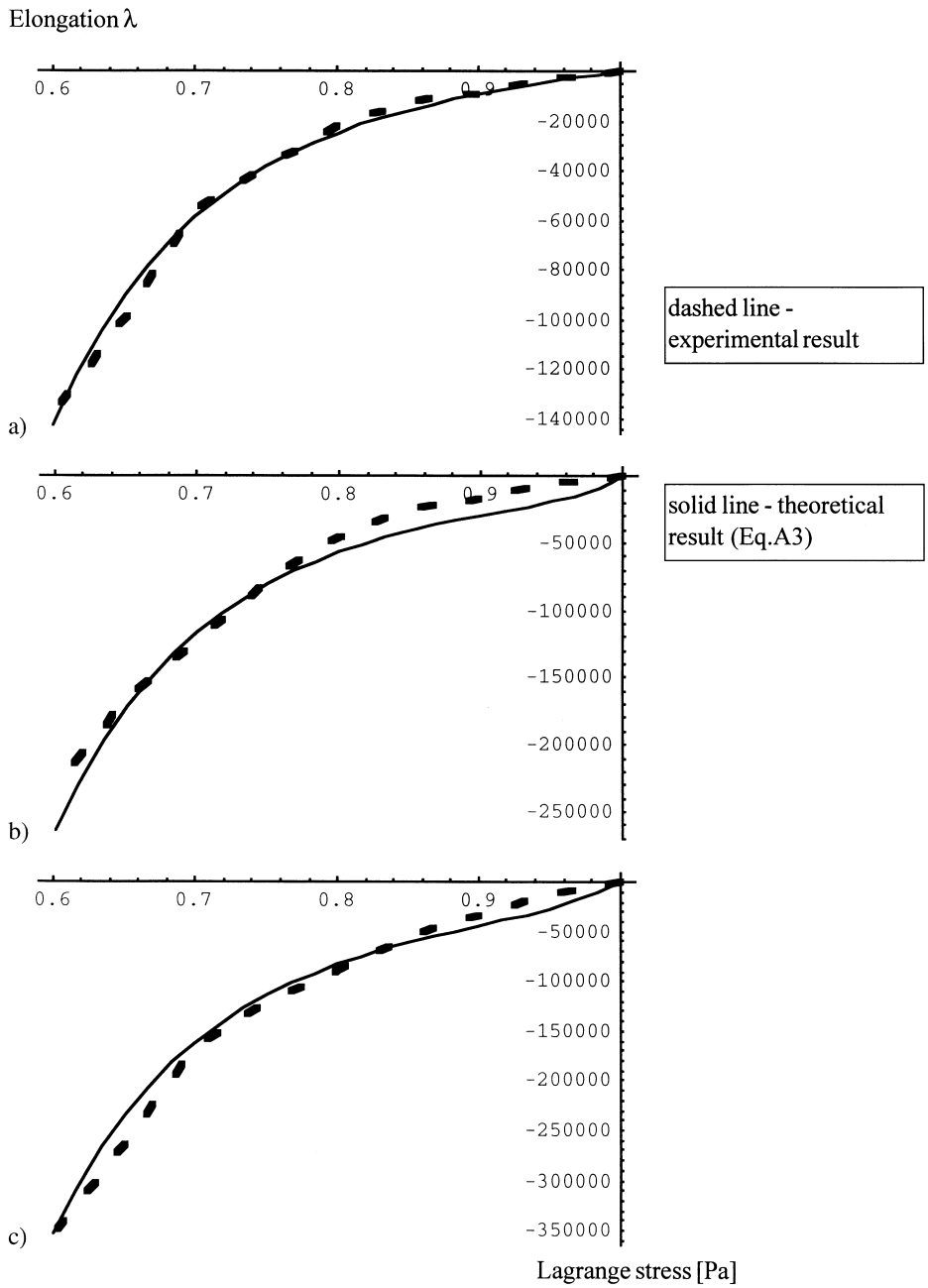

Fig. 1. Lagrange stress–elongation (λ) relations for Rhesus monkey liver tissue, experimental and theoretical results: (a) loading speed 5 cm s^{-1}, corresponding to the strain rate of about 0.225 s^{-1}, (b) loading speed 250 cm s^{-1}, corresponding to the strain rate of about 11.25 s^{-1}, (c) loading speed 500 cm s^{-1}, corresponding to the strain rate of about 22.50 s^{-1}.

the best of author's knowledge, the only published data on in vivo deformation behaviour of liver and kidney. The experiments where designed so that the injury mechanisms could be observed. The organ was laid onto a load cell while still being perfused by the living animal. Load and impactor displacement were measured. In the calculation of stresses Melvin et al. approximated the test configuration as that of an uniaxial compression.

From the perspective of this study, the most valuable results are the stress–strain curves obtained for various loading velocities (Figs. 1 and 2) and estimates of strain energy densities (Table 3). The loading velocities were 5, 250 and 500 cm s^{-1} which corresponded to the nominal strain rates of approximately 0.225, 11.25 and 22.5 1 s^{-1} for the liver, and 0.385, 19.24, 38.47 1 s^{-1} for the kidney. Melvin's result should be understood as average across

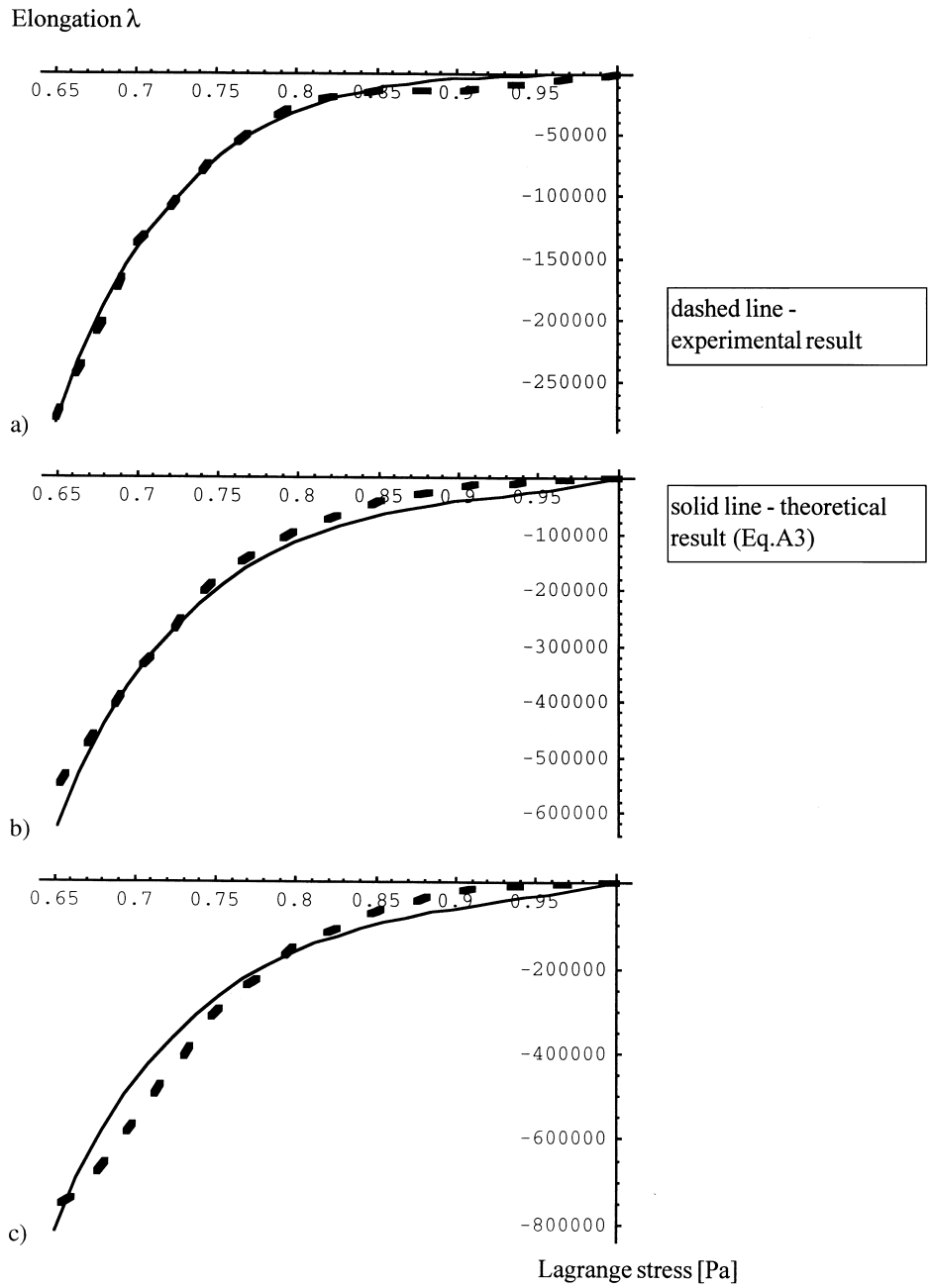

Fig. 2. Lagrange stress–elongation (λ) relations for Rhesus monkey kidney tissue, experimental and theoretical results: (a) loading speed 5 cm s^{-1}, corresponding to the strain rate of about 0.385 s^{-1}, (b) loading speed 250 cm s^{-1}, corresponding to the strain rate of about 19.24 s^{-1}, (c) loading speed 500 cm s^{-1}, corresponding to the strain rate of about 38.47 s^{-1}.

the organs, since the tests were performed on the organs in vivo, not on tissue samples extracted from the specific locations.

The stress–strain curves are convex for all compression rates containing no linear portion from which a meaningful elastic modulus could be determined. The tissue response stiffened with the increasing loading speed, indicating a strong stress–strain rate dependence. The results shown in Figs. 1 and 2 are in general agreement with those published in (Farshad et al., 1998). It needs to be pointed out here, that for slower strain rates there is no other data available for comparisons.

3. Determination of material constants of hyper-viscoelastic constitutive model for liver and kidney

To model the deformation behaviour of liver and kidney, the hyper-viscoelastic constitutive equation developed originally for brain tissue (Miller and Chinzei,

1997) was used. Therefore only a very brief description is given below.

The model is based on a strain energy function with time-dependent coefficients, written in the form of convolution integral:

$$W = \int_0^t \left\{ \sum_{i+j=1}^{N} C_{ij}(t-\tau) \frac{\mathrm{d}}{\mathrm{d}\tau} [(J_1 - 3)^i (J_2 - 3)^j] \right\} \mathrm{d}\tau, \quad (1)$$

where

$$C_{ij} = C_{ij\infty} + \sum_{k=1}^{n} C_{ijk} \mathrm{e}^{-1/\tau_k} \quad (2)$$

describe mechanical properties of the tissue, J_1 and J_2 are the first and second strain invariants, and τ_k are characteristic times. N is the order of polynomial in strain invariants, used for strain energy function description.

Based on our experiences with modelling brain tissue, in this work the following simplifying assumptions were adopted:

- the isotropy of the tissue in the unloaded state
- tissue incompressibility (see e.g. Farshad et al., 1998; Schmidlin et al., 1996)

Since the test conditions approximated those of uniaxial compression with the tissue being free to expand laterally under load, additional assumption of orthogonality of deformation was adopted. This assumption is crucial because it allows the derivation of stress–elongation (λ_z) dependency in analytical form

The above assumptions allow computation of the only non-zero Lagrange stress components from the simple formula (Miller and Chinzei, 1997):

$$T_{zz} = \int_0^t \left\{ \sum_{i+j=1}^{N} C_{ij}(t-\tau) \frac{\mathrm{d}}{\mathrm{d}\tau} \left[\frac{\partial}{\partial \lambda_z} ((J_1 - 3)^i (J_2 - 3)^j) \right] \right\} \mathrm{d}\tau. \quad (3)$$

It is important to note that the expression for stresses (3) is linear in material parameters $C_{ij\infty}$ and C_{ijk}, see Eq. (2). Eq. (3) served as a basis for the comparison of the theory and experiment.

In order to identify material coefficients in Eq. (3) additional simplifications were necessary. The character of the stress–strain curves for liver and kidney is very similar to those of brain tissue, so the same assumptions which lead to the estimation of material constants for brain tissue (Miller and Chinzei, 1997) were adopted here. The second-order polynomial strain function was taken. The equality of the energy of reciprocal deformation to that of the original one (see Mooney, 1940; Miller and Chinzei, 1997) was assumed: $C_{01}/C_{10} = 1$ and $C_{02}/C_{20} = 1$. For simplicity C_{11} was taken to be equal to zero. For the range of loading strain rates considered, it was sufficient to use only one time-dependent term in the C_{ij} expansion ($n = 1$ in e.g. 2). Incorporation in the model of a larger number of time-dependent terms would result in the necessity of identifying considerably more corresponding material coefficients. The time constants $t_1 = 0.002$ s was chosen basing on the nominal strain rates in experiments and the considerations for the brain (Mendis et al., 1995). The estimated strain rates in experiments of Melvin et al. (1973) were similar to those of Estes and MacElhaney (1970) for brain sample tests. The time constant used by Mendis et al. for brain modelling, based on the experiments of Estes and MacElhaney was 0.008 s. However, due to the contribution of time dependent terms to the stresses at the lowest strain rate considered, Mendis et al. had to decrease the values of estimated equilibrium coefficients. Therefore, in this study the time constant is taken smaller than that used by Mendis et al. As a result, the contribution of time dependence to the model predictions for slowest experiments is negligible.

The adoption of the above assumptions results in the following equation for stress:

$$\begin{aligned} T_{zz} = \int_0^t \Big\{ & C_{10}(t-\tau) \frac{\mathrm{d}}{\mathrm{d}\tau} (2\lambda_z - 2\lambda_z^{-2}) \\ & + C_{01}(t-\tau) \frac{d}{\mathrm{d}\tau} (-2\lambda_z^{-3}) \\ & + C_{20}(t-\tau) (\lambda_z^2 + 2\lambda_z^{-1} - 3) \frac{\mathrm{d}}{\mathrm{d}\tau} (2\lambda_z - 2\lambda_z^{-2}) \\ & + C_{02}(t-\tau) (\lambda_z^{-2} + 2\lambda_z - 3) \frac{\mathrm{d}}{\mathrm{d}\tau} (-2\lambda_z^{-3}) \Big\} \mathrm{d}\tau \quad (4) \end{aligned}$$

with four material constants to be identified: $C_{10\infty} = C_{01\infty}$, $C_{20\infty} = C_{02\infty}$, $C_{101} = C_{011}$ and $C_{201} = C_{021}$. In the case of the compression with constant velocity, the integral (4) can be evaluated analytically, see the Appendix.

Function *Regress*, available in Mathematica software package (Wolfram Research, 1996), was used to find least square fit to the slow test data. The influence of the exponentially decaying terms on the results of the slow test is very small, so that during the procedure of determining equilibrium coefficients $C_{10\infty} = C_{01\infty}$, $C_{20\infty} = C_{02\infty}$, the remaining coefficients were set to zero. This does not imply that the tissue exhibits elastic behaviour at strain rates of 0.2–0.3 s^{-1} but that the model proposed here is not capable of capturing viscoelastic behaviour at lower strain rates. It must be noted here that there is no experimental data available on liver and kidney tissue deformation behaviour at lower strain rates.

After setting the values of $C_{10\infty}$ and $C_{20\infty}$ the remaining coefficients C_{101} and C_{201} were calculated through a simultaneous least-squares fit to the medium and fast speed experimental results.

Table 1
Liver material coefficients and multiple correlation coefficients

Equilibrium (slow test results used)	Characteristic time $t_1 = 0.002$ s (medium and fast speed test results used)
$C_{10\infty} = C_{01\infty} = 6206$ Pa; $R^2 = 0.996$	$C_{101} = C_{011} = 57413$ Pa; $R^2 = 0.974$
$C_{20\infty} = C_{02\infty} = 3492$ Pa; $R^2 = 0.996$	$C_{201} = C_{021} = 9730$ Pa; $R^2 = 0.974$

Table 2
Kidney material coefficients and multiple correlation coefficients

Equilibrium (slow test results used)	Characteristic time $t_1 = 0.002$ s (medium and fast speed test results used)
$C_{10\infty} = C_{01\infty} = 898$ Pa; $R^2 = 0.9975$	$C_{101} = C_{011} = 63278$ Pa; $R^2 = 0.983$
$C_{20\infty} = C_{02\infty} = 26368$ Pa; $R^2 = 0.9975$	$C_{201} = C_{021} = 65662$ Pa; $R^2 = 0.983$

4. Results

Table 1 contains the values of estimated material coefficients for liver tissue together with multiple correlation coefficients characterising the quality of fit. The corresponding values for the kidney are presented in Table 2.

The prediction of the constitutive model and the experimental results are shown in Figs. 1 and 2. The agreement between the theoretical model and the experimental results is good. As an additional test of the appropriateness of the proposed model the values of the strain energy density function (Eq. (1)) were calculated and compared with those estimated by Melvin et al. (1973) for maximum strains (see Table 3). The agreement is very good for all but two cases. A weaker match for medium speed loading for kidney and slow loading for liver results from very low forces at small strains detected by Melvin et al.

5. Discussion and conclusions

In this study the mathematical models of liver and kidney tissue deformation behaviour are presented. They are based on in vivo compression experimental results. The tissues exhibit non-linear, stress–strain relations as well as strong dependence between stresses and strain rates.

The use of the single-phase, hyper-viscoelastic model based on the concept of the strain energy function, in the form of convolution integral with coefficient expressed in the form of exponential series is advocated. Agreement between the proposed theoretical model and experiment is good for compression levels reaching 35% and for loading velocities varying over two orders of magnitude.

It is well known that changes in impact velocity greatly affect the injury level (Rouhana et al., 1985; Viano and Lau, 1988). The inclusion of the stress–strain rate dependence in the constitutive model provides means to model such behaviour.

The mathematical models presented here are useful in approximate modelling the behaviour of abdominal organ tissues, which includes spatial averaging of material properties. The strain rate range investigated ($> 0.2\ s^{-1}$) ascertains that the model is meaningful in car crash or other situations leading to impacts at high speeds. At the same time, rather high estimated values of equilibrium coefficients $C_{ij\infty}$ make the model unsuitable for applications to low strain rate deformations. Similar procedure can lead to constructing a constitutive model for applications in surgical simulations. However, the experimental results concerning the deformation behaviour of abdominal organs at low strain rates (say $0.01\ s^{-1}$, typical for neurosurgery) are not available yet.

Before the finite element simulation of liver and kidney deformation is conducted, further research is needed to determine the way these organs are attached to the body. Such knowledge is necessary to formulate properly the boundary conditions for the mathematical formulation of the problem.

Acknowledgements

The financial support of the Australian Research Council is gratefully acknowledged.

Table 3
Strain energy density: experimental versus theoretical results (Eq. (1))

	Loading speed (strain rate)	Maximum compressive nominal strain	Strain energy density (experiment) (J)	Strain energy density (theoretical results) (J)
Kidney	5 cm s^{-1}(0.385 s^{-1})	35%	23 500	20 278
	250 cm s^{-1}(19.24 s^{-1})	43.25%	108 500	141 068
	500 cm s^{-1}(38.47 s^{-1})	37.5%	93 000	97 183
Liver	5 cm s^{-1}(0.225 l s^{-1})	53.5%	34 500	57 290
	250 cm s^{-1}(11.25 l s^{-1})	49%	50 750	69 342
	500 cm s^{-1}(22.5 l s^{-1})	48.88%	65 000	66 336

Appendix A

The expression for the Lagrange stress can be divided into two parts: time independent T_0, and time dependent, with characteristic time τ_1, T_1. In case of unconfined compression with constant velocity the integral in Eq. (8) can be evaluated analytically. The result was obtained using Mathematica (Wolfram, 1996) software package:

$$T_0 = C_{10\infty}\left(4 + 2(-1+\lambda_z) - \frac{2}{\lambda_z^3} - \frac{2}{\lambda_z^2}\right) + C_{20\infty}\left(-8 + 8(-1+\lambda_z) + 12(-1+\lambda_z)^2 + 4(-1+\lambda_z)^3 - \frac{4}{\lambda_z^5} + \frac{4}{\lambda_z^3} + \frac{8}{\lambda_z^2}\right), \tag{A.1}$$

$$\begin{aligned} T_1 = C_{101}\Bigg(&\frac{E^{1/v\tau_1((-1-\lambda_z)/v\tau_1)}\,\text{ExpIntegralEi}\,[-1/v\tau_1]\,(1-2v\tau_1)}{v^3\tau_1^3} \\ &- \frac{E^{\lambda_z/v\tau_1}\text{ExpIntegralEi}[-\lambda_z/v\tau_1]\,(1-2v\tau_1)}{v^3\tau_1^3} + E^{-(1-\lambda_z)/v\tau_1}\,\frac{(1-3v\tau_1+4v^2\tau_1^2+2v^3\tau_1^3)}{v^2\tau_1^2} \\ &+ \frac{1}{V^2\lambda_2^3\tau_1^2}\,(-1+3v\tau_1-4v^2\tau_1^2-2v^3\tau_1^3+2v^3(1-\lambda_z)^3\tau_1^3 \\ &- (1-\lambda_z)^2\,(1-2v\tau_1-6v^3\tau_1^3)+(1-\lambda_z)\,(2-5v\tau_1+2v^2\tau_1^2+6v^3\tau_1^3))\Bigg) \\ &+ C_{201}\Bigg[\frac{E^{1/v\tau_1-1-\lambda_z/v\tau_1}\,\text{ExpIntegralEi}\left[-\frac{1}{v\tau_1}\right](1-12v^2\tau_1^2+48v^3\tau_1^3)}{6v^5\tau_1^5} \\ &- \frac{E^{\lambda_z/v\tau_1}\,\text{ExpIntegralEi}\left[-\frac{\lambda_z}{v\tau_1}\right](1-12v^2\,\tau_1^2+48v^3\,\tau_1^3)}{6v^5\,\tau_1^5} + \frac{1}{6v^4\,\tau_1^4} \\ &\left(E^{-(1-\lambda_z)/v\tau_1}(1-v\tau_1-10v^2\,\tau_1^2+54v^3\,\tau_1^3-48v^4\,\tau_1^4+48v^5\,\tau_1^5+14\,4v^6\,\tau_1^6+14\,4v^7\,\tau_1^7)\right) \\ &+ \frac{1}{6v^4\lambda_z^5\tau_1^4}\,(-1+v\tau_1+10v^2\tau_1^2 \\ &- 54v^3\tau_1^3+48v^4\tau_1^4-48v^5\tau_1^5+72v^5(1-\lambda_z)^7\,\tau_1^5-144v^6\,\tau_1^6-144v^7\,\tau_1^7 \\ &- 72v^5(1-\lambda_z)^6\,\tau_1^5(7+2v\tau_1)+48v^5(1-\lambda_z)^5\,\tau_1^5(31+18v\tau_1+3v^2\tau_1^2)+(1-\lambda_z) \\ &\times(4-3v\tau_1-44v^2\tau_1^2+222v^3\tau_1^3-192v^4\tau_1^4+384v^5\tau_2^5+864v^6\tau_1^6+720v^7\tau_1^7) \\ &- (1-\lambda_z)^4(1-12v^2\tau_1^2+48v^3\tau_1^3+2400v^5\tau_1^5+2160v^6\tau_1^6+720v^7\tau_1^7) \\ &- (1-\lambda_z)^2(6-3v\tau_1-70v^2\tau_1^2+324v^3\tau_1^3 \\ &- 168v^4\tau_1^4+1272v^5\tau_2^5+2160v^6\tau_1^6+1440v^7)+(1-\lambda_z)^3 \\ &(4-v\tau_1-48v^2\tau_1^2+204v^3\tau_1^3-48v^4\tau_1^4+2280v^5\tau_1^5+2880v^6\tau_1^6+1440v^7\tau_1^7))\Bigg] \end{aligned} \tag{A.2}$$

where v is a loading velocity divided by the initial height. ExpIntegralEi denotes exponential integral function.

$$T_{zz} = T_0 + T_1. \tag{A.3}$$

References

Brett, P.N., Fraser, C.A., Henningan, M., Griffiths, M.V., Kamel, Y., 1995. Automatic Surgical Tools for Penetrating Flexible Tissues. IEEE Engineering Medicine in Biology, 264–270.

Burdea, G., 1996. Force and Touch Feedback for Virtual Reality. Wiley, New York.

Divicenti, F.C., Rives, J.D., Laborde, E.J., Fleming, I.D., Cohn Jr., I., 1968. Blunt Abdominal trauma, Journal Trauma. 8 (6), 1004–1013.

Estes, M.S., McElhaney J.H., 1970. Response of brain tissue of compressive loading, ASME Paper No. 70-BHF-13.

Farshad, M., Barbezat, M., Schmidlin, F., Bidaut, L., Niederer, P., Graber, P., 1998. Material Characterization and mathematical modelling of the pig kidney in relation with biomechanical analysis of renal trauma. Proceedings of North American Congress on Biomechanics. Waterloo, Ontario, Canada.

Guerriero, G., 1993. Traumatic injury to the kidney and ureter. Current Opinion in Urology 3, 186–193.

Hossak, D.W., 1972. The pattern of injuries received by 500 drivers and passengers killed in road accidents. Medical Journal of Australia 2, 193–195.

Huelke, D.F., Melvin, J.W., 1980. Anatomy, injury frequency, biomechanics, and human tolerances. SAE Transactions 800098, pp. 633–651.

Melvin, J.W., Stalnaker, R.L., Roberts, V.L., 1973. Impact injury mechanisms in abdominal organs, SAE Transactions 730968, pp. 115–126.

Mendis, K.K., Stalnaker, R.L., Advani, S.H., 1995. A constitutive relationship for large deformation finite element modeling of brain tissue. Transactions ASME, Journal of Biomechanics Engineering 117, 279–285.

Miller, K., Chinzei, K., 1997. Constitutive modelling of brain tissue; experiment and theory. Journal of Biomechanics 30 (11/12), 1115–1121.

Mooney, M., 1940. A theory of large elastic deformation. Journal of Applied Physics 11, 582–592.

Rouhana, S.W., Lau, I.V., Ridella, S.A., 1985. Influence of velocity and forced compression on the severity of abdominal injury in blunt, nonpenetrating lateral impact. Journal of Trauma 25, 490–500.

Rutledge, R., Thomason, M., Oller, D., Meredith, W., Moylan, J., Clancy, T., Cunningham, P., Baker, C., 1991. The spectrum of abdominal injuries associated with the use of seat belts. Journal of Trauma 31, 820–826.

Schmidlin, F.R., Schmid, P., Kurtyka, T., Iselin, C.E., Graber, P., 1996. Force transmission and stress distribution in a computer simulated model of the kidney: an analysis of the injury mechanisms in renal trauma. Journal of Trauma 40, 791–796.

Viano, D.C., King, A.I., Melvin, J.W., Weber, K., 1989a. Injury biomechanics research: an essential element in the prevention of trauma. Journal of Biomechanics 22 (5), 403–417.

Viano, D.C., Lau, I.V., 1988. A viscous tolerance criterion for soft tissue injury assessment. Journal of Biomechanics 21 (5), 387–399.

Viano, D.C., Lau, I.V., Asbury, C., 1989b. Biomechanics of the human chest, abdomen, and pelvis in lateral impact. Accident Analyses and Prevention 21 (6), 553–574.

Wolfram, S., 1996. Mathematica Book. 3rd edition Wolfram Media, Cambridge University Press, USA, pp. 816–820.

Wolfram Research, 1996. Mathematica 3.0 Standard Add-on Packages. Wolfram Media, Cambridge University Press, USA, pp. 428–439.

Yamada, H., 1970. Strength of Biological Materials. The Wiliams & Wilkins Company, Baltimore, USA.